


 Cite this: *RSC Adv.*, 2020, 10, 18908

# Green biorefinery – the ultra-high hydrolysis rate and behavior of *Populus tomentosa* hemicellulose autohydrolysis under moderate subcritical water conditions†

 Yanru Xu,<sup>a</sup> Pengfei Wang,<sup>a</sup> Shiwen Xue,<sup>a</sup> Fangong Kong,<sup>b</sup> Hao Ren<sup>\*ab</sup> and Huamin Zhai<sup>\*a</sup>

A high monosaccharide conversion rate of hemicellulose in a green solvent and under moderate reaction conditions for industrialization is one of the most important keys in a lignocellulosic biorefinery. The behavior of *Populus tomentosa* hemicellulose polysaccharides, crystallinity and the furfural formation in the autohydrolysis process under moderate subcritical water conditions (160–180 °C, 0.618–1.002 MPa) were studied. The results have shown that the hemicellulose was converted to corresponding monosaccharides at an ultra-high hydrolysis rate. Factor analysis indicates that the temperature is the most important factor affecting hemicellulose autohydrolysis. When the autohydrolysis temperature increased from 160 to 180 °C for 2 h, the hydrolysis rate of xylose, rhamnose, galactose, mannose, and glucose from hemicellulose increased from 70% to 91%, 71% to 100%, 82% to 95%, 42% to 58%, and 34% to 37%, respectively. Arabinose was completely dissolved in 30 min. The xylose, rhamnose, galactose, and arabinose from hemicellulose could be almost completely removed under the conditions. The hemicellulose removal rate obtained herein exceeded the values reported for most acid, alkali, ionic liquid, or deep eutectic solvent treatments. It is notable that almost all glucose in hemicellulose was dissolved and the glucose in cellulose was partially hydrolyzed. An analysis of the sugar composition and the crystallinity change in the process at 180 °C demonstrate that hydrolysis reaction started to shift from amorphous regions to crystalline regions, due to the partial hydrolysis of crystalline cellulose after 90 min at 180 °C. Overall, these results show that the moderate subcritical water autohydrolysis of hemicellulose in *Populus tomentosa* may be a potential bio-refinery process.

 Received 13th March 2020  
 Accepted 11th May 2020

DOI: 10.1039/d0ra02350g

[rsc.li/rsc-advances](http://rsc.li/rsc-advances)

## 1 Introduction

The continuous global economy and technology development results in a growing demand for energy, which, in turn, necessitates the search for new green energy sources to replace fossil fuels in view of the unsustainability of the latter and the environmental pollution caused by their use.<sup>1</sup> In this regard, biomass has attracted much attention as the only sustainable and currently used carbon resource suited to meet humanity's chemical and material needs.<sup>2</sup> The conversion of biomass into materials of diverse types and functions is a complex process requiring the efficient separation of lignocellulosic biomass components (cellulose, hemicellulose, and lignin) and their conversion to value

added products.<sup>3</sup> However, the high resistance of lignocellulosic biomass to biological degradation leads to low conversion efficiency, by product formation, and high energy consumption, restricting the widespread use of biomass as a raw material.<sup>4</sup> The ongoing development of industrial technology in the world has inspired extensive research on modern biomass conversion methods and the associated key scientific problems.

Traditional methods of lignocellulose component separation employ acids, alkali, organic solvents, and ionic liquids as catalysts.<sup>5</sup> For example, Si *et al.* studied the hydrolysis of bamboo fiber promoted by a novel sulfonated cross linked chitosan solid acid catalyst in an ionic liquid containing Tween 80, PEG 4000, or sodium dodecyl sulfate as surfactants. The results showed that Tween 80 was the most effective surfactant, allowing one to achieve a total reducing sugar yield of 68.01% after 24 h at 120 °C.<sup>6</sup> Wu studied the enzymatic hydrolysis of wheat straw using a two-step process combining wheat straw autohydrolysis pretreatment with alkali post treatment. The results showed that at 180 °C, maximum glucose and xylan conversions equaled 19.2% and 64.6%, respectively.<sup>7</sup> Zhai *et al.*

<sup>a</sup>Jiangsu Provincial Key Lab of Pulp and Paper Science and Technology, Nanjing Forestry University, Address No. 159 LongPan Road, Nanjing, JiangSu Province, 210037, China. E-mail: renhao@njfu.edu.cn; hzhai@njfu.edu.cn

<sup>b</sup>State Key Laboratory of Biobased Material and Green Papermaking, Qilu University of Technology, Shandong Academy of Sciences, Jinan, 250353, China

† Electronic supplementary information (ESI) available. See DOI: 10.1039/d0ra02350g



studied the inhibitory effects of carbocation scavengers on cellulase catalyzed slurry hydrolysis of sulfuric acid pretreated black pine, demonstrating that cellulose hydrolysis rate increased from 41% to 54% upon the addition of eugenol, with the corresponding yields of arabinose, galactose, glucan, xylan, and mannose determined as 0.1%, 0.1%, 55.4%, 1.4%, and 2%, respectively.<sup>8</sup> To sum up, although traditional methods allow lignocellulosic to effectively separate, transform, and utilize high added value components to a certain extent, the use of catalysts results in equipment corrosion and poses the problem of poor catalyst recovery. Thus, the above disadvantages make the investigation of the separation and high value added utilization of lignocellulose components under green conditions a task of high practical importance.<sup>9</sup>

Water, which is the most environmentally friendly, safe, and low cost solvent in the chemical industry,<sup>10</sup> may be used as a medium only for certain green organic reactions, *i.e.*, features a rather limited application scope. Supercritical water refers to a state obtained at a temperature and pressure exceeding those of the critical point (374 °C and 22.1 MPa),<sup>11</sup> whereas subcritical water (SCW) refers to liquid water at a temperature between its atmospheric pressure boiling point (100 °C) and the critical point (374 °C), and is also known as ultra-hot or hot pressed water.<sup>12</sup> Both subcritical and supercritical water exhibit unique tunable properties similar to those of organic solvents and can be used to depolymerize woody fiber biomass in biological refining,<sup>13</sup> as exemplified by Željko's and María's review.<sup>14,15</sup> Mood *et al.* measured changes in the contents of total reducing sugars and each monosaccharide in bamboo treated with SCW at 170–220 °C, demonstrating that the highest yields of reducing sugars (42.21%), xylan (21.9%), and arabinose (9.23%) were obtained at 180 °C, while the yield of glucose was maximized (16.3%) at 220 °C.<sup>16</sup> Lachos-Perez *et al.* studied the SCW mediated hydrolysis of sugarcane straw at 190–260 °C and 9–16 MPa, demonstrating that the highest yields of glucose (2.1%), xylan (2.3%), galactose (0.7%), and arabinose (1.0%) were obtained at 200 °C/10 MPa.<sup>17</sup> Juliana *et al.* used the SCW mediated hydrolysis of sugarcane bagasse to produce fermentable sugar at 20 MPa and 213 °C, 251 °C, and 290 °C. The highest lignocellulose decomposition and hydrolysis efficiencies were observed at 290 °C, with the highest yields of arabinose, galactose, glucose, and xylose equaling 0.95%, 0.13%, 1.78%, 0.12%, and 1.8%, respectively.<sup>18</sup> Abaide *et al.* prepared fermentable sugars and biological products by semi-continuous hydrolysis of straw with SCW at 25 MPa and 180 °C, 220 °C, or 260 °C, showing that the maximum reducing sugar content of 33.4% was obtained at 260 °C. The highest hydrolysis extent was observed at 220 °C, with the maximum contents/conversions of the thus obtained xylose, arabinose, and glucose equaling 7.81%/92.19%, 4.85%/95.15%, and 1.54%/98.46%, respectively.<sup>19</sup> Guan *et al.* employed single factor and orthogonal experiments to determine the best conditions for the pretreatment of sawdust by high temperature liquid water as follows: temperature 185 °C, substrate loading 11 wt%, and reaction time 13 min. Under these conditions, glucose and xylose were obtained in yields of 29.49% and 20.53%, respectively. After pretreatment, cellulose, hemicellulose and lignin conversions were determined as 21.39%, 85.41%, and 4.55%,

respectively.<sup>20</sup> However, many of the above methods employ highly complex equipment and feature high energy consumption and high cost, being poorly suited for the SCW mediated separation and application of lignocellulose components.

In summary, although the dissolution of biomass components has been extensively investigated, efficient conversions of xylose, arabinose, mannose, and other lignocellulose monosaccharides could be achieved only at temperatures and pressures above 200 °C and 20 MPa, respectively. Thus, to realize the efficient dissolution of monosaccharides in the whole biomass and industrial scale biomass refining based on green solvent usage, one should increase the efficiency and lower the cost of biomass refining.

Up to now, the study of biorefinery shows that the cell wall composition of fast growing *poplar* (*Populus tomentosa*) is similar to that of trees and grasses. In addition, compared with gramineous plant resources, the fiber morphology and microstructure of hardwood are simpler, and the cell composition is relatively single. Therefore, on the basis of existing research, we herein consider *poplar* as a raw material for hydrolysis to establish more moderate and efficient biological refining conditions. The unique properties of subcritical and supercritical water make these green solvents well suited for low cost and environmentally friendly industrial scale biomass treatment. Herein, we investigated the autohydrolysis of hemicellulose in *poplar* wood by moderate SCW at 160–180 °C and 0.618–1.002 MPa. The exploration of xylose and arabinose, rhamnose, mannose and galactose, glucose under different conditions of dissolution laws, revealed the moderate subcritical hydrolysis degree of *poplar* hemicellulose from behavior and the influence of the hydrolysis rate limit, and thus establish a moderate subcritical hemicellulose hydrolysis degree monosaccharide components from the regulatory mechanism of hydrolysis of dissolution.

## 2 Experimental

### 2.1 Material

*Poplar* (*Populus tomentosa*) was provided from Anyang city, in Henan province, China. The raw material was smashed into powder (100–150 mesh) by a laboratory pulverizer and dried in oven at 60 °C for 24 h.

Methanol, ethanol, benzene, glacial acetic acid, sulfuric acid, acetone, and NaOH were analytically pure (Nanjing Chemical Reagent Co., Ltd.), Sodium chlorite (analytical pure) was procured from Shanghai McLean biochemical technology co. LTD. Sodium borohydride (analytical pure) was procured from Sinopharma chemical reagent co. LTD. Acetic anhydride (analytical pure) was procured from Shanghai lingfeng chemical reagent co. LTD. Barium hydroxide (analytical pure) was procured from Xilong chemical reagent co. LTD.

### 2.2 Chemical constituent analysis of *Populus tomentosa* wood powder

The compositional analysis of *poplar* was measured according to the National Renewable Energy Laboratory (NREL) method.<sup>21</sup> Specifically, the klason lignin, acid soluble lignin, benzene-alcohol extractive and ash were determined according to



Table 1 Chemical composition of *poplar* wood powder

Chemical composition	Content (%)
Total lignin	26.8
Klason lignin	24.0
Acid soluble lignin	2.8
Holocellulose	73.9
Alpha-cellulose	47.1
Rhamnose	0.3
Arabinose	1.1
Xylose	17.1
Mannose	2.5
Galactose	1.1
Glucose	50.9
Benzene-alcohol extractive	1.9
Ash content	0.5

standard methods, namely: NREL/TP-510-42618, NREL/TP-510-42619, NREL/TP-510-42622, respectively.

The monosaccharide composition was determined using gas chromatography (GC) equipment and the basis of the methodology presented in the literature.<sup>22</sup> The gas chromatography equipped with a SH-Rtx-1701 capillary column (30 mL × 0.32 mm × 0.1 μm) and a FID detector. The temperature program functioned as follows: oven temperature was initially set at 160 °C, then increased to 250 °C and was then held at 250 °C for 55 min. The heater temperatures of both the injector and detector were kept at 230 °C. Nitrogen was used as the carrier gas. The results were reported as the relative peak areas. Rhamnose, xylose, mannose, galactose, arabinose and glucose were used as monosaccharide standards, according to the ref. 22. The chemical composition and monosaccharide contents of wood powder (dry material) are shown in Table 1.

### 2.3 Autohydrolysis

*Poplar* powder and distilled water are mixed evenly in a covered and closed steel autoclave with a volume of 1.25 L according to the solid–liquid ratio of 1 : 10 (g : mL), and then the closed steel autoclave is heated in the oil bath digester. The mixture was allowed to stand at room temperature for 30 min for *poplar* powder to fully soak and then heated to 160 °C, 170 °C, or 180 °C at a rate of 2 °C min<sup>-1</sup> and kept at this temperature for 0 min, 30 min, 60 min, 90 min, or 120 min. The reaction pressure is used at the saturated vapor pressure corresponding to the reaction temperature. Subsequently, the reaction mixture was filtered through a 300 mesh pulp bag to separate the autohydrolysis residue from the corresponding solution. The residue was washed with tap water until the pH of washings became neutral and then air dried to balance the moisture for analysis.

### 2.4 Analysis

#### 2.4.1 Determination of chemical constituents in hydrolyzates

**2.4.1.1. Determination of solid content.** 30 mL hydrolyzate aliquot was transferred to a weighing bottle and oven baked at 105 °C to constant weight. The solid content  $S$  (g L<sup>-1</sup>) was calculated as:

$$S = \frac{W_c}{0.03} \times 100\%$$

where  $W_c$  is the mass of the solid residue (g) obtained after baking.

**2.4.1.2. Determination of furfural content.**<sup>23</sup> According to ref. 23, in a concentrated acetic acid medium, furfural have an isosbestic point at 276 nm, acid soluble lignin is the main interference in the determination of furfural spectrum. Acid-soluble lignin was absorbed in the spectral range of 250 nm to 500 nm, while furfural were not absorbed after 325 nm. Finally, based on the wavelength of isosbestic point (276 nm) and the maximum absorption wavelength of furfural (272 nm), as well as the wavelength of acid-soluble lignin at 325 nm (furfural was absorbed), the content of furfural in the extract of the material could be quantitatively detected by a simple three-wavelength method.

Furfural content ( $c$ ) was determined from absorbances at 272, 276, and 325 nm (converted to the same dilution factor  $R$ ), denoted as  $A_{272}$ ,  $A_{276}$ , and  $A_{325}$ , respectively:

$$c = \frac{A_{272} - 0.88A_{276} - 0.41A_{325}}{23.61} \times R$$

**2.4.1.3. Determination of reducing sugar content.**<sup>24</sup> Using 3,5-dinitrosalicylic acid (DNS) method to determine the reducing sugar. Xylose was employed as a substrate to establish the marking line and draw the standard curve. After measurement, the standard xylose curve was obtained as  $y = 16.87x - 0.1003$ ,  $R^2 = 0.9997$ . The concentration of reducing sugar was calculated according to the standard curve.

**2.4.2 Calculation of removal rate.** The removal rate ( $R$ ) of each component<sup>25</sup>

$$R = \left(1 - \frac{m}{M}\right) \times 100\%$$

where  $m$  is the residual content of a chemical component after autohydrolysis treatment (g), and  $M$  is the content of this component in 60 g of absolutely dry raw material (g).

**2.5.1 Determination of crystallinity.** The XRD patterns were recorded in an Ultima IV X-ray diffraction (Shimadzu) operating with Cu K $\alpha$  radiation ( $\lambda = 0.154$  nm) with angle range of 5–40° at a step of 0.02°. The analysis was performed on dried pulverized samples. Using XRD analysis, the crystallinity of the samples was calculated according to peak intensity method. Fiber crystallinity  $X$  was calculated as

$$X = \frac{I_{002} - I_{am}}{I_{002}} \times 100\%$$

where  $I_{002}$  and  $I_{am}$  are the diffraction intensity of 002 crystal face and amorphous region, respectively.

## 3 Results and discussion

### 3.1 Effect of hydrolysis degree (temperature and time) on pH of autohydrolysis system

Hardwood hemicellulose is mainly composed of *O*-acetyl-4-*O*-methylglucuronyl- $\beta$ -D-xylan (as shown in Fig. 2). Xylan is the most important component of hardwood hemicellulose. Its



main chain is composed of  $\beta$ -xylopyranosyl connected by 1,4- $\beta$ -glucoside bond, and its branches are mainly 4-*O*-methylglucuronyl, acetyl and arabinose.<sup>26</sup> After the heating process, the reaction system reached 160 °C, 170 °C and 180 °C respectively from room temperature, and then kept the corresponding temperature unchanged to carry out different reaction time (30 min, 60 min, 90 min, 120 min). Fig. 1 shows the change of pH with reaction time at 160 °C, 170 °C, and 180 °C. The curve trend observation can be divided into two stages: rapid pH decline was observed at 0–30 min, while slow decline was observed after 30 min, in agreement with the findings of Chen *et al.*<sup>27</sup> In the fast stage, pH rapidly decreased from 5.0 to 4.1 when the reaction temperature equaled 160 °C, while declines from 4.6 to 3.9 and from 4.4 to 3.8 were observed at 170 °C and 180 °C, respectively. In the slow stage, hemicellulose degradation gradually tended to equilibrium, and pH slowly decreased to 3.9, 3.8, and 3.6 at 160 °C, 170 °C, and 180 °C, respectively.

Fig. 1 shows that when the reaction time is 0 min, the pH value of three different reaction temperatures drops rapidly from the original neutral of 7.0 to 5.0, 4.6 and 4.4 respectively, which indicates that in the process of temperature rise, due to the rise of temperature and pressure, water molecules are in subcritical state, resulting in the change of state and physical and chemical properties of water: ① the relative permittivity is reduced, subcritical water becomes weak polar solvent, and the reaction rate is accelerated;<sup>28</sup> ② the increase of ion product and the decrease of hydrogen bond between water molecules result in the high concentration of hydrogen ions and hydroxyl ions;<sup>29,30</sup> ③ the reduction of viscosity and surface tension of water is conducive to mass transfer and permeation, thus increasing the reaction rate. Therefore, in the process of heating up, the ionization balance of neutral water is destroyed, and the  $H^+$  concentration in the reaction system gradually increases, so that the acetyl group, glycoaldehyde acid group and other branch chains on hemicellulose take the lead in acid hydrolysis

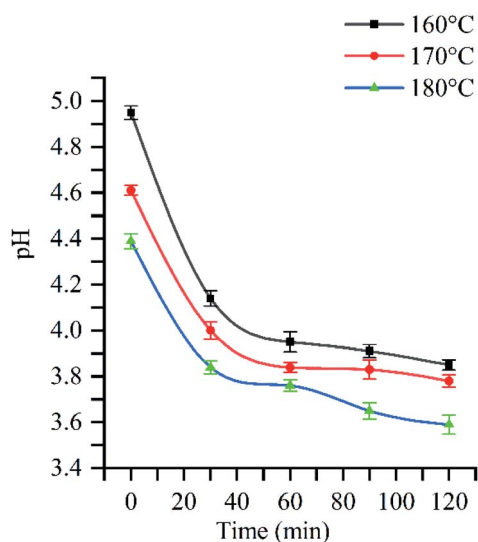


Fig. 1 The influence of reaction temperature and time on pH of hydrolysate.

and fall off, forming acetic acid. The production of acetic acid continues to reduce the pH value of solution, leading to the breaking of glycoside bond in hemicellulose, and promoting the degradation of hemicellulose.<sup>31,32</sup> With the extension of reaction time, hemicellulose degradation will continue, so the acetic acid produced by side chain fracture plays a catalytic role in the autohydrolysis reaction.<sup>33</sup> In this reaction, time and temperature are the main factors affecting pH value.<sup>34</sup> The influence of temperature and time on the pH value of autohydrolysis occurs in the whole process of hydrolysis. The effects of reaction temperature were most pronounced at 180 °C: pH value after the heat preservation time 30 min slowly downhill solution phase can still decline at a faster pace, show the hemicellulose in 180 °C under the condition of cell wall degradation over time is still constantly, is a growing acidic hydrolysis system. When the temperature is 180 °C, the pressure is 15.75 MPa, and the reaction time is 120 min, the pH value of the hydrolysate drops to 3.6, which is the same as that of “when the temperature is lower than 230 °C at the end of hemicellulose degradation, the pH value range of the hydrolysate can reach 3.2–3.8”.<sup>35–37</sup> It shows that the hemicellulose decreases under the subcritical condition of relatively low temperature (180 °C). The solution can reach a higher level.

In conclusion, the hydrolysis degree of hemicellulose is affected by the pressure, reaction temperature, reaction time and pH value of reaction system. The hydrolysis effect of hemicellulose increases with the increase of reaction temperature, reaction time and pressure. Meanwhile, the hydrolyzate pH reduction was critical for the removal of other components such as small molecular weight lignin, an amorphous region of cellulose, and was thus very important.

### 3.2 Effect of hydrolysis temperature and time on monosaccharide removal

**3.2.1 Xylose.** Hemicellulose is a mixture of heteropolysaccharide containing pentose and hexose. Xylose is the main monosaccharide of hemicellulose of *poplar*. Meanwhile, related studies show that furfural is the main decomposition product of xylose.<sup>39</sup> Fig. 3a shows the change of xylose removal rate with reaction time at 160 °C, 170 °C and 180 °C. From the curve trend, the hydrolysis process of xylose showed a stage change. At 160 °C, xylose removal could be divided into slow removal (0–60 min), rapid/main removal (60–90 min), and supplementary removal (>90 min) stages, in which xylose removal rate increased from 1% to 22%, from 22% to 61%, and from 61% to 70%, respectively. At 170 °C, xylose removal could be divided into rapid removal (0–60 min) and supplementary removal (>60 min) stages, in which xylose removal rate increased from 5% to 62% and from 62% to 83%, respectively. At 180 °C, xylose removal could also be divided into rapid (0–30 min) and supplementary (>30 min) removal stages, in which xylose removal rate increased from 7% to 78% and from 78% to 91%, respectively, subsequently saturating.

Fig. 3a shows that temperature strongly influenced the rate of xylose removal as well as the maximum removal rate and the time distribution of each stage. When the reaction temperature



is 160 °C, the maximum removal rate of xylose is 70%. It can be seen from Fig. 1 that at this time, the acidity of the autohydrolysis is weak, and the glycoside bond is partially broken, that is, the degradation rate of hemicellulose is low, resulting in the low removal rate of xylose. When the reaction temperature is 180 °C, the maximum removal rate of xylose is 91%, the acidity in the solution is strong, and the increase of H<sup>+</sup> can promote the breaking of pentoside bond of xylan and the conversion of xylose removal to furfural,<sup>40</sup> which is consistent with the change rule of furfural (3.2.4).

**3.2.2 Rhamnose.** Fig. 3b shows the change of rhamnose removal rate with reaction time at 160 °C, 170 °C and 180 °C. From the curve trend, rhamnose and xylose exhibited similar autohydrolysis trends (Fig. 2a and b). At 160 °C, rhamnose removal could be divided into slow removal (0–30 min), rapid/main removal (30–90 min), and supplementary removal (>90 min) stages, in which rhamnose removal rate increased from 4% to 9%, from 9% to 71%, and from 71% to hydrolysis equilibrium, respectively. At 170 °C, rhamnose removal could be divided into rapid removal (0–60 min) and supplementary removal (>60 min) stages, in which rhamnose removal rate increased from 6% to 89% and from 89% to 100%, respectively (rhamnose could only be detected in trace amounts in the raw material). At 180 °C, rhamnose removal could also be divided into rapid (0–30 min) and supplementary (>30 min) removal stages, in which rhamnose removal rate increased from 22% to 88% and from 88% to 100% (after 60 min), respectively. In conclusion, increasing temperature can improve the rate of rhamnose removal and shorten the complete removal time of rhamnose from 120 min to 60 min.

**3.2.3 Arabinose.** In the process of autohydrolysis, arabinose was more easily hydrolyzed than xylose and rhamnose.<sup>41</sup> Fig. 3c shows the change of arabinose removal rate with reaction time at 160 °C, 170 °C and 180 °C. According to the removal law of other pentoses, from the curve trend, arabinose in Fig. 3c was all in the supplementary removal stage at the holding stage of 160 °C, 170 °C, and 180 °C, and the removal rate increased slowly from 54%, 64%, and 87%, respectively, and was completely removed at 120 min, 60 min and 30 min, respectively.

Fig. 3c shows that increasing the reaction temperature can improve the removal rate of arabinose. Arabinose and rhamnose in hemicellulose are the branches of xylan main chain. It can be seen from Fig. 3a–c that when the reaction time is 0 min, the removal rate of xylose in pentose is the lowest. At the same time, the markedly low pH observed at this reaction time (Fig. 1) indicated that during autohydrolysis, the branched chains of hemicellulose were preferentially cleaved to produce acetic acid,

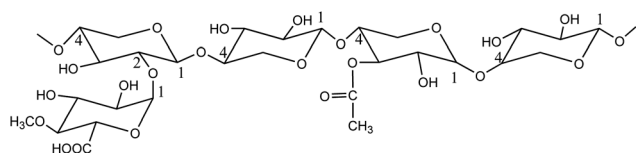


Fig. 2 O-Acetyl-4-O-methylglucuronyl- $\beta$ -D-xylan.<sup>38</sup>

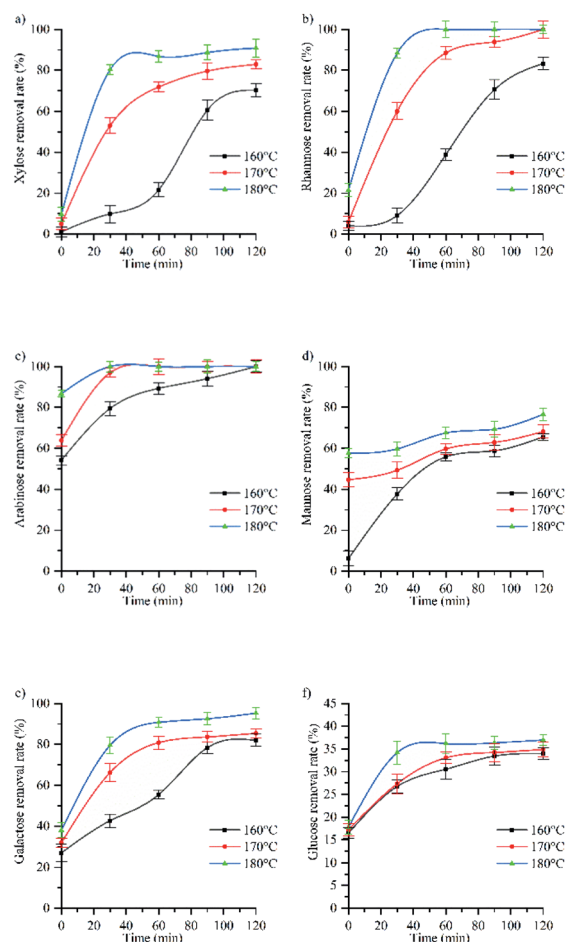


Fig. 3 The influence of temperature and time on removal rate of (a) xylose, (b) rhamnose, (c) arabinose, (d) mannose, (e) galactose, (f) glucose.

arabinose, rhamnose, and glucuronic acid. Therefore, the hydrolysis rate of various monosaccharides is arabinose, rhamnose and xylose. The results show that the hydrolysis rate of monosaccharide is directly proportional to its removal efficiency,<sup>42</sup> in a study on a hydrolysis model of the three pentoses, the fastest hydrolysis was observed for methyl pyran arabinose with glycosylates in hemicellulose,<sup>43</sup> which led to the complete removal of arabinose at 160 °C, while rhamnose could be completely removed at 170 °C. To sum up, increasing the temperature can make the slow removal stage and the fast removal stage complete the reaction rapidly during the heating process, and improve the removal rate of arabinose, that is, the complete removal time is shortened from 120 min to 30 min.

**3.2.4 Mannose.** Mannose, galactose, and glucose are hexoses, the acid hydrolysis property of glycosidic bond determines the hydrolysis rate of monosaccharide. Because hexoside bond is more difficult to hydrolyze than pentose bond,<sup>44</sup> most hexose hydrolysis rate is slower than that of pentose.

Fig. 3d shows the change of mannose removal rate with reaction time at 160 °C, 170 °C and 180 °C. From the curve trend, the hydrolysis process of mannose showed a stage change. At 160 °C, mannose removal could be divided into rapid



removal (0–30 min) and supplementary removal (>30 min) stages, in which mannose removal rate increased from 6% to 41% and from 41% to hydrolysis equilibrium, respectively. The obtained trend indicated that a certain time was required to reach hydrolysis equilibrium. At 170 °C and 180 °C, the supplementary removal stage started from 0 min, and the removal rate slowly increased with time from 42% to 58%. Notably, the predicted equilibrium state was not reached after 120 min.

According to Fig. 3d, when the reaction time is 0 min, the removal rate at 170 °C (44%) was seven times higher than that at 160 °C (6%), which was ascribed to the special distribution of mannose in hemicellulose and the fact that the corresponding links are easy to break only at temperatures above 160 °C.<sup>45</sup> Therefore, temperature strongly influenced mannose removal rate. And when the temperature is 180 °C and the reaction time is 120 min, the mannose removal rate does not reach the equilibrium state, so it is speculated that increasing the reaction temperature or time can further improve the mannose removal rate.

**3.2.5 Galactose.** Although galactose belongs to the class of hexoses, which are more stable than pentoses, its water solubility is higher than those of other hexoses.<sup>46</sup> Under the autohydrolysis conditions employed herein, the dissolution behavior of galactose resembled that of pentoses.

Fig. 3e shows the change of galactose removal rate with reaction time at 160 °C, 170 °C and 180 °C. From the curve trend, the hydrolysis process of galactose showed a stage change.

At 160 °C, galactose removal could be divided into slow removal (0–60 min), rapid removal (60–90 min), and supplementary removal (>90 min) stages, in which galactose removal rate increased from 27% to 50%, from 50% to 82%, and from 82% to hydrolysis equilibrium, respectively. At 170 °C, galactose removal could be divided into rapid removal (0–60 min) and supplementary removal (>60 min) stages, in which galactose removal rate increased from 32% to 80% and from 80% to 85%, respectively, finally reaching an equilibrium value. At 180 °C, rapid removal (0–60 min) and supplementary removal (>60 min) stages were identified, during which galactose removal rate increased from 38% to 90% and from 90% to 95%, respectively, before reaching equilibrium. It can be seen from Fig. 4 that when the reaction temperature rises from 160 °C to 180 °C, the mannose removal rate rises from 82% to the maximum of 95%. Therefore, the mannose removal rate increases with the increase of reaction temperature and time.

**3.2.6 Glucose.** As glucose is mainly contained in cellulose, which has a very stable crystalline zone, the behavior of this hexose was different from those of other monosaccharides.

Fig. 3f shows the change of glucose removal rate with reaction time at 160 °C, 170 °C and 180 °C. From the curve trend, the hydrolysis process of glucose showed a stage change. At 160 °C, glucose removal could be divided into rapid removal (0–60 min) and slow removal (60–120 min) stages, during which glucose removal rate increased from 16.51% to 31% and from 31% to 34%, respectively. At 170 °C, rapid removal (0–60 min) and equilibrium (>60 min) stages were observed, during which glucose removal rate increased from 16.51% to 33% and from

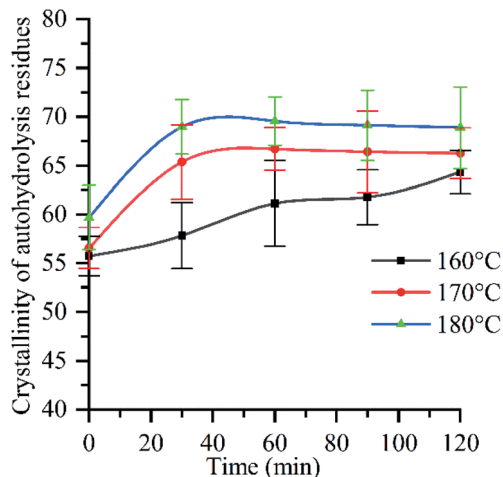


Fig. 4 The influence of hydrolysis degree and hemicellulose removal rate on crystallinity of autohydrolysis residues.

33% to 35%, respectively. At 180 °C, rapid removal (0–30 min), supplementary removal (30–90 min), and deep removal (>90 min) stages were detected, during which glucose removal rate increased from 18% to 33%, from 33% to 36%, and from 36% to 37% (after 120 min).

In pulping and papermaking field, it is generally believed that the cellulose content is approximately equal to the  $\alpha$ -cellulose content (47.1%), but since the cellulose content is composed of cellulose and anti-alkaline degradation hemicellulose, the estimated cellulose content using the Alpha-cellulose content is slightly higher than the actual content of cellulose. It can be seen from Table 1 that the holocellulose content is 73.8%, and the holocellulose content is generally the sum of cellulose and hemicellulose (containing a small amount of lignin). Therefore, the holocellulose content minus  $\alpha$ -cellulose content can be approximately considered as the hemicellulose content (26.8%). At the current research stage, we assumed that the glucose content in hemicellulose was approximately equal to the total glucan content in the raw material composition analysis minus the content of  $\alpha$ -cellulose (3.8%). Based on the values of other hemicellulose polysaccharides in Table 1, we finally calculated that the glucose proportion of hemicellulose polysaccharides in hemicellulose was about 14.2%. According to the difference between holocellulose and  $\alpha$ -cellulose, the content of hemicellulose was estimated to be 26.8% in this study. However, a small amount of lignin had not been removed in the actual preparation process of holocellulose, so the content of glucose in the actual hemicellulose was higher than 14.2%. X. M. Zhang *et al.* extracted hemicellulose from carbohydrates with *poplar* as raw material. The analysis showed that there were about 14.1–19.06% glucose in hemicellulose.<sup>38</sup> In this experiment, when the reaction temperature is 160 °C and the reaction time is 0 min, the glucose removal rate is 16.51%. Therefore, it can be estimated that about 16% of the glucose in the hemicellulose used in this paper is glucose. This part of glucose was preferentially removed during hemicellulose hydrolysis and glucose as it is connected



with pentose. At the same time, it can be seen from Fig. 1 that hemicellulose has been degraded at 0 min, so when the reaction time is 0 min, glucose in hemicellulose is degraded. However, when hemicellulose was hydrolyzed to a certain extent, the removal of glucose contained in cellulose was relatively slow because of the stability of the cellulose crystalline region and its high content. Glucose removal mostly occurred in the amorphous region of cellulose, however, with the increase of temperature and the gradual decrease of pH (Fig. 1), the increase of  $H^+$  concentration causes the degradation of glucose in the crystalline region of cellulose. When the reaction temperature is 180 °C and the reaction time is 90 min, the removal rate of glucose increases from 36% to 37%, which is due to the increase of temperature and pressure, which affects the properties of water,<sup>47</sup> while the properties of water affect the maximum concentration and dissolution rate of monosaccharide, so temperature and pressure affect the removal rate of monosaccharide. At 180 °C, the saturated vapor pressure of water is 10 bar, and its viscosity is half that at 100 °C, which is conducive to mass transfer and permeation, thus improving the reaction rate.<sup>48</sup> Therefore, water at 180 °C was more likely to attack fibers, while enhanced mass transfer between cell walls resulted in a hemicellulose removal degree of 90%, which led to the continuous decrease of hydrolyzate pH to promote the degradation of crystalline cellulose. From Fig. 3f, it can be inferred that at the reaction temperature of 180 °C and the reaction time of 90 min, the crystalline cellulose region began to degrade after 90 min at 180 °C, in agreement with the crystallinity change (3.3 and ESI Fig. 1†).

### 3.3 Effect of hydrolysis degree on crystallinity

In the process of autohydrolysis, due to the increase of temperature, hemicellulose is degraded, resulting in acid solution, while hemicellulose contains more amorphous regions, and a large number of removal will lead to the increase of crystallinity.<sup>49,50</sup> During *poplar* autohydrolysis, degradation of cellulose I amorphous regions through the attack of hydronic ions increased cellulose crystallinity and exposed highly stable crystalline cellulose, which is not easily invaded by water molecules.<sup>51</sup> Steam generated at high temperature also causes the thermal degradation of cellulose. Ordinary hot water pretreatment can only provide a small amount of amorphous cellulose for thermal degradation, which is mainly in the form of low glucan.<sup>47</sup>

In this paper, only the change of monosaccharide content in the hydrolysate is tested, while the removal of glucose comes from cellulose and hemicellulose. Therefore, the minimum value of hemicellulose removal rate is calculated based on the sum of the change of monosaccharide content in xylose, rhamnose, arabinose, mannose and galactose and the estimated ratio of hemicellulose content. Considering that the dehydration correction coefficients of pentose and hexose in the conversion of monosaccharide and total sugar are 0.88 and 0.9 respectively, it can be calculated that the hemicellulose content of each 60 g hydrolysis raw material in this experiment is about 13.764 g; according to Fig. 3, when the temperature is 180 °C

and the reaction time is 120 min, the removal rates of xylose, rhamnose, arabinose, mannose and galactose in hemicellulose are 89%, 100%, 100%, 77% and 95% respectively, and the sum of their masses is 10.7615 g, so the lowest conservative estimate of hemicellulose removal rate is about 78%.

It is generally believed that the hemicellulose of hardwood consists of two kinds of polysaccharides: glucuronoxylan and glucomannan, in which glucose mainly exists in glucomannan; glucan is the main component of cellulose, but in some tree species, a small amount of glucan also exists in the form of xyloglucan, accounting for only about 20% of the primary wall of plant cell.<sup>52–54</sup> In this paper, only glucose in the form of glucomannan is considered in the evaluation of the degree of hemicellulose removal. The ratio of glucose to mannose is generally 1 : 1 or 1 : 2 in glucomannan.<sup>55</sup> Assuming that the ratio of hemicellulose glucose to mannose is 1 : 1, when the temperature is 180 °C and the reaction time is 120 min, the total mass of xylose, rhamnose, arabinose, mannose, galactose and glucose in hemicellulose is 11.8010 g, and the hemicellulose removal rate is 86%. In conclusion, the removal rate of hemicellulose can reach 78–86% under the condition of autohydrolysis without any catalyst and low pressure. Although the hemicellulose removal rate reported in previous studies is higher than that in this study, for example, J. sun *et al.* under the subcritical water system with corn straw as raw material and 4% sulfuric acid as catalyst, when the reaction temperature is 180 °C and the reaction time is 20 minutes, the hemicellulose removal rate is 95.9%.<sup>56</sup> X. Jiang *et al.* used *poplar* as raw material and 10 g L<sup>-1</sup> NaOH as catalyst in the alkaline solution system. When the reaction temperature was 180 °C and the reaction time was 20 minutes, the hemicellulose removal rate was 87.82%.<sup>57</sup> However, this experiment was carried out without any catalyst, with only green solvent water and low pressure.

Raw material crystallinity significantly increased after autohydrolysis (Fig. 4), following a trend similar to that of hydrolysis rate (ESI Fig. 4a†), which indicated that the crystallinity of raw materials was closely related to the removal of chemical components. When the reaction time is 0 min, the crystallinity of different reaction temperature is 56% (160 °C), 57% (170 °C), 60% (180 °C) respectively, which are higher than the crystallinity of raw materials. The reason is that the increase of  $H^+$  concentration in the reaction system during the heating process causes the degradation of hemicellulose and the increase of crystallinity.<sup>58</sup> Due to the increase of pressure, reaction temperature and time, the interaction force between water molecules is weakened, hydrogen bond is broken, and the ionization rate of water molecules is accelerated, which makes the  $H^+$  concentration in the reaction system continuously increase,<sup>30</sup> and the pH value continuously decreases, resulting in the increase of hemicellulose hydrolysis rate and the increase of crystallinity of autohydrolyzed residue. When the reaction temperature is 180 °C and the reaction time is 90 min, the pH value of the solution is 3.65, and the crystallinity reaches 70% of the maximum value. After the reaction time is 90 min, the pH value of the reaction system continues to decrease due to the increase of the reaction time (Fig. 1). The amorphous region of cellulose I will be attacked and degraded by hydroionization,



exposing the crystalline region of cellulose, resulting in the destruction of the crystalline region of cellulose,<sup>59</sup> therefore, the crystallinity of autohydrolyzed residue decreased. At the same time, it can be seen from Fig. 3f that the glucose removal rate has an upward trend in the deep removal stage (see Section 3.2.6), which proves that the cellulose crystal zone is destroyed (The relationship between hemicellulose removal rate and crystallinity see ESI Section 1†). In conclusion, when the reaction temperature is 180 °C and the reaction time is 90 min, the cellulose crystal zone begins to be destroyed. It is a key step towards biorefinery that crystal zone is destroyed to depolymerize tissue and cell polymers.

### 3.4 Effect of hydrolysis degree on furfural production

Fig. 5 shows the change process of furfural content with reaction time under three different reaction temperatures of 160 °C, 170 °C and 180 °C. From the curve trend, at 160 °C, furfural concentration slowly increased from 0.08 g L<sup>-1</sup> to 0.41 g L<sup>-1</sup>; at 170 °C, furfural production could be divided into slow growth (0–90 min) and accelerated growth (>90 min) stages. In the former stage, furfural concentration uniformly increased from 0.14 g L<sup>-1</sup> to 0.62 g L<sup>-1</sup>; At 180 °C, furfural production could also be divided into slow growth (0–30 min) and accelerated growth (>30 min) stages, in which furfural concentration increased from 0.23 g L<sup>-1</sup> to 0.32 g L<sup>-1</sup> and from 0.32 g L<sup>-1</sup> to 2.69 g L<sup>-1</sup>, respectively.

It can be seen from Fig. 5 that the content of furfural in the hydrolysate increases with the prolongation of holding time. When the reaction temperature is 160 °C and the reaction time is 120 min, the furfural concentration is 0.41 g L<sup>-1</sup>, and about 3% of the pentose is converted into furfural. Because the acidity of the reaction system is weak at this time, furfural is more easily generated under the condition of strong acidity,<sup>60</sup> most of the monosaccharides obtained from hemicellulose hydrolysis are difficult to convert into furfural. When the temperature is

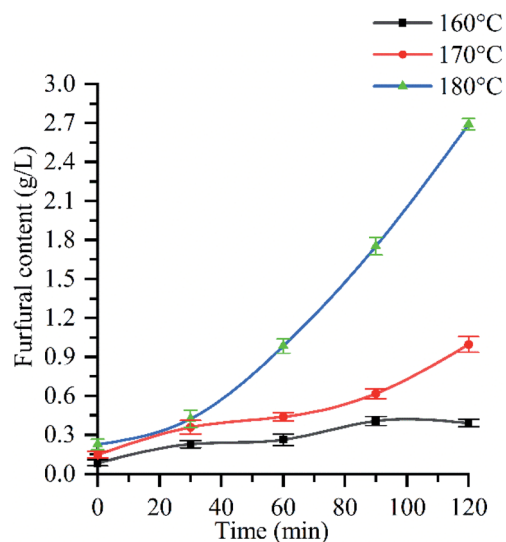


Fig. 5 The influence of temperature and time on furfural concentration.

170 °C and the reaction time is 120 min, the furfural concentration is 0.99 g L<sup>-1</sup>, about 28% of the pentose is converted into furfural. When the temperature is 180 °C and the reaction time is 120 min, the maximum concentration of furfural (2.69 g L<sup>-1</sup>) can reach three times of that at 170 °C (0.99 g L<sup>-1</sup>), and about 40% of pentose can be degraded to furfural. It can be seen from Fig. 3f and 1 that after 90 min, the glucose in cellulose begins to be partially removed, and the removal rate of monosaccharide is the highest at 120 min. At the same time, the acidity of the reaction system is the strongest, which promotes the formation of furfural, so the furfural concentration increases rapidly after 90 min. This corresponds to the change rule of crystallinity (see Section 3.3) and reducing sugar (ESI Fig. 2†).

In conclusion, the furfural concentration is affected by the pressure, reaction temperature, reaction time and pH value of the autohydrolysate. With the increase of pressure, reaction temperature and reaction time, the pH value of the autohydrolysate decreases, which promotes the dehydration of monosaccharide, leading to the increase of furfural concentration. Therefore, when the reaction temperature is 180 °C, the pressure is 1.002 MPa, and the reaction time is 120 min, the pH of the autohydrolysate is 3.6, the acidity is the strongest, the hemicellulose hydrolysis effect is the best, and the furfural concentration is the largest (2.69 g L<sup>-1</sup>), at this time, about 40% of the pentose is degraded to furfural. Morais A. R. C. *et al.* studied the hydrolysis of wheat straw in water/organic solvent (THF/MIBK) biphasic system under subcritical water.<sup>61</sup> The results showed that under the conditions of initial CO<sub>2</sub> pressure of 50 bar, temperature of 180 °C and reaction time of 60 min, the largest amount of furfural produced by hemicellulose hydrolysate was 44%. Prado J. M. *et al.* studied the hydrolysis of bagasse under subcritical conditions. The results showed that when the temperature was 290 °C and the reaction time was 30 min, the maximum content of hemicellulose furfural was 10%.<sup>18</sup> In contrast, the conversion of furfural to 40% can reach a high level under the subcritical condition of relatively low temperature (180 °C).

## 4 Conclusions

Study on the behavior of *poplar* hemicellulose autohydrolysis under moderate subcritical water conditions was conducted. It was found that the ultra-high hydrolysis rate of *poplar* hemicellulose was obtained by the autohydrolysis under the conditions. For temperatures of 160–180 °C, and the removal rate of xylose, rhamnose, arabinose, mannose, and glucose increased with increasing reaction time in 2 hours. At a temperature of 180 °C and a reaction time of 2 h, the removal rate of xylose, rhamnose, arabinose, galactose, and glucose in hemicellulose exceeded 90%, and the removal rate of rhamnose and arabinose were close to 100%.

In this study, under the condition of no catalyst and low pressure, when the temperature is 180 °C and the reaction time is 120 min, the removal rate of hemicellulose can reach 78–86%.

The relationship between hemicellulose hydrolysis rate, glucose production rate and crystallinity in the process at 180 °C was comprehensively analyzed, which proved that the





autohydrolysis reaction started the transition from amorphous zone to crystalline zone under such conditions. It can be expected that further moderate temperature increase in the subcritical water range may lead to further depolymerisation of cellulose aggregation, hydrolysis of a large amount of cellulose into glucose. It may further move towards the green biorefinery. Further work is under way.

It is demonstrated that the formed reducing sugar was converted into furfural by comparing and analyzing the relationship between the reducing sugar formation, change and the furfural formation between 160–180 °C. The conversion rate from the reducing sugar into the furfural was closely related to temperature. An approximately 40% of the reducing sugar by hydrolysis at 180 °C for 2 h was converted to the furfural. Such a high conversion rate is extremely advantageous for biorefinery. Compared with the existing biorefinery solvent system, this study achieved a higher conversion of furfural at a relatively low temperature without any catalyst addition.

Our studies have provided evidence that *poplar* hemi-cellulose autohydrolysis under moderate subcritical water conditions could be a green biorefinery process.

## Abbreviations

SCW	Subcritical water
<i>Poplar</i>	<i>Populus tomentosa</i>
PEG	Polyethylene glycol
DNS	Dinitrosalicylic acid

## Author contributions

H. R. and H. M. Z. conceived the idea and supervised the project. H. R., H. M. Z. and Y. R. X. designed the research. Y. R. X. carried out most of the experiments and analyzed the data. P. F. W., S. H. W. and W. C. participated in the experiments. H. R., H. M. Z., Y. R. X. and P. F. W. discussed the results and prepared the manuscript. S. W. X. and F. G. K. provided some useful suggestions.

## Conflicts of interest

There are no conflicts to declare.

## Acknowledgements

The project supported by NSFC (31600474), the foundation (No. KF201803) of state key laboratory of biobased material and green papermaking, Qilu University of Technology, Shandong Academy of Sciences. The authors are also grateful for the support of the National Key Basic Research Program of China (Project No. 2018NFUSPITP670 and No. 201710298039Z). The work was also supported by the Nanjing Forestry University Outstanding Youth Fund (NLJQ2015-5). The research did not receive any specific Grant from funding agencies in the public, commercial, or not-for profit sectors.

## References

- 1 R. Hao and L. Zhu, *Wood Sci. Technol.*, 2018, 1–19.
- 2 W. H. Zhang, I. Kaur, W. Zhang, S. Jing and Y. Ni, *Sep. Purif. Technol.*, 2017, **188**, 508–511.
- 3 N. Feng, L. Guo, H. Ren, Y. Xie, Z. Jiang, M. Ek and H. Zhai, *Int. J. Biol. Macromol.*, 2019, **122**, 210–215.
- 4 G. Tian, Y. Fu, J. Zhuang, Z. Wang and Q. Li, *Bioresour. Technol.*, 2017, **237**, S096085241730130X.
- 5 E. D. Jong and R. J. A. Gosselink, *Bioenergy research: advances and applications*, Elsevier, 2014, pp. 277–313.
- 6 W. Si, Y. Li, J. Zheng, S. A. Wei and D. Wang, *Carbohydr. Polym.*, 2017, **174**, 154–159.
- 7 X. Wu, C. Huang, S. Zhai, C. Liang, C. Huang, C. Lai and Q. Yong, *Bioresour. Technol.*, 2017, **251**, 374–380.
- 8 R. Zhai, J. Hu and J. N. Saddler, *Bioresour. Technol.*, 2018, **258**, 12.
- 9 H. Passos, M. G. Freire and J. A. P. Coutinho, *Green Chem.*, 2015, **46**, 4786–4815.
- 10 A. J. Ragauskas, C. K. Williams, B. H. Davison, B. George, C. John, C. A. Eckert, W. J. Frederick, J. P. Hallett and C. L. Liotta, *Science*, 2006, **311**, 484–489.
- 11 F. M. Gírio, C. Fonseca, F. Carvalho, L. C. Duarte, S. Marques and R. Bogel-Lukasik, *Bioresour. Technol.*, 2010, **101**, 4775–4800.
- 12 J. Zhang, C. Wen, J. Gu, C. Ji, Y. Duan and H. Zhang, *Int. J. Biol. Macromol.*, 2019, **123**, 1002–1011.
- 13 M. Muharja, F. Junianti, D. Ranggina, T. Nurtono and A. Widjaja, *Bioresour. Technol.*, 2018, **249**, 268–275.
- 14 Ž. Knez, M. K. Hrnič, M. Čolnik and M. Škerget, *J. Supercrit. Fluids*, 2018, **133**, 591–602.
- 15 M. J. Cocero, Á. Cabeza, N. Abad, T. Adamovic, L. Vaquerizo, C. M. Martínez and M. V. Pazo-Cepeda, *J. Supercrit. Fluids*, 2018, **133**, 550–565.
- 16 M. Mohan, T. Banerjee and V. V. Goud, *Bioresour. Technol.*, 2015, **191**, 244–252.
- 17 D. Lachos-Perez, G. A. Tompsett, P. Guerra, M. T. Timko, M. A. Rostagno, J. Martínez and T. Forster-Carneiro, *Bioresour. Technol.*, 2017, **243**, 1069–1077.
- 18 J. M. Prado, L. A. Follegatti-Romero, T. Forster-Carneiro, M. A. Rostagno, F. M. Filho and M. A. A. Meireles, *J. Supercrit. Fluids*, 2014, **86**, 15–22.
- 19 M. Alboofetileh, M. Rezaei, M. Tabarsa, S. G. You and G. Cravotto, *Int. J. Biol. Macromol.*, 2019, **128**, 244–253.
- 20 G. Dongming, C. Luxia, Z. Yue and X. Zhenghao, *Taiyangneng Xuebao*, 2017, **38**, 2001–2004.
- 21 B. H. A. Sluiter, R. Ruiz, C. Scarlata, J. Sluiter, D. Templeton and D. Crocker, *Laboratory analytical procedure*, 2008, vol. 1617, pp. 1–16.
- 22 L. G. Borchardt and C. V. Piper, *Tappi*, 1970, **53**, 257–260.
- 23 C. Zhang, X. Chai, X. Luo, S. Fu and H. Zhan, *Spectrosc. Spectral Anal.*, 2010, **30**, 247–250.
- 24 G. Hou, N. J. Feng, L. Zhang, K. Dai, Q. Wang, H. Zhai and X. Hua, *J. Nanjing For. Univ.*, 2014, **38**, 113–117.
- 25 C. Qing, *J. Agric. Sci. Technol.*, 2015, **17**, 70–79.



- 26 J. Huang, L. Wu, H. Tong, Z. Liu, C. He and G. Pan, *J. Fuel Chem. Technol.*, 2016, **44**, 911–920.
- 27 C. Xiaowen, L. Martin and H. Adriaan Van, *Bioresour. Technol.*, 2010, **101**, 7812–7819.
- 28 N. Yoshii, S. Miura and S. Okazaki, *Chem. Phys. Lett.*, 2001, **345**, 195–200.
- 29 G. Brunner, *J. Supercrit. Fluids*, 2009, **47**, 373–381.
- 30 N. Akiya and P. E. Savage, *Chem. Rev.*, 2002, **102**, 2725–2750.
- 31 J. Li, M. Zhang and D. Wang, *Bioresour. Technol.*, 2018, **263**, 232–241.
- 32 Q. Sun, Extraction and Separation of Hemicelluloses from Poplar and Its Preliminary Application, PhD thesis, Qilu University of Technology (Shandong Academy of Sciences), Jinan, 2018.
- 33 F. M. Yedro, H. Grénman, J. V. Rissanen, T. Salmi, J. García-Serna and M. J. Cocero, *J. Supercrit. Fluids*, 2017, **129**, 56–62.
- 34 H. Ren, P. Wang and H. Zhai, *Chem. Ind. For. Prod.*, 2019, **39**, 65–71.
- 35 T. E. Amidon, C. D. Wood, A. M. Shupe, Y. Wang, M. Graves and S. Liu, *J. Biobased Mater. Bioenergy*, 2008, **2**, 100–120.
- 36 W. W. Al-Dajani, U. W. Tschirner and T. Jensen, *Tappi J.*, 2009, **8**, 30–37.
- 37 K. Leppänen, P. Spetz, A. Pranovich, K. Hartonen, V. Kitunen and H. Ilvesniemi, *Wood Sci. Technol.*, 2011, **45**, 223–236.
- 38 X. Zhang, L. Meng, F. Xu and R. Sun, *Ind. Crops Prod.*, 2011, **33**, 310–316.
- 39 N. Paksung and Y. Matsumura, *Ind. Eng. Chem. Res.*, 2015, **54**, 7604–7613.
- 40 H. Pińkowska, P. Wolak and A. Złocińska, *Biomass Bioenergy*, 2011, **35**, 3902–3912.
- 41 Y. Zhang, Y. Fu, Z. Wang and M. Qin, *Transactions of China Pulp and Paper*, 2015, pp. 1–5.
- 42 K. K. Encinas-Soto, A. R. Martín-García and M. Perez-Tello, *Ind. Eng. Chem. Res.*, 2015, **55**, 1–13.
- 43 S. Machmudah, H. Kanda and M. Goto, in *Water Extraction of Bioactive Compounds*, Elsevier, 2017, pp. 69–107.
- 44 P. Khuwijtjaru, T. Kobayashi and S. Adachi, *J. Carbohydr. Chem.*, 2016, **35**, 286–299.
- 45 A. Romero, D. Cantero, A. Nieto-Márquez, C. Martínez and M. J. Cocero, *Green Chem.*, 2016, **18**, 1–14.
- 46 Y. Zhao, D. Li, W. Lu, H. Wang and X. Pu, *Acta Chim. Sin.*, 2008, **66**, 2295–2301.
- 47 P. Li, Y. Chao, C. Chen and Q. Meng, *Trans. China Pulp Pap.*, 2012, **31**, 1–6.
- 48 C. Zhu, L. Guo, H. Jin, Z. Ou, W. Wei and J. Huang, *Int. J. Hydrogen Energy*, 2018, **43**, 14078–14086.
- 49 M. F. Li, C. Z. Chen and R. C. Sun, *Cellulose*, 2014, **21**, 4105–4117.
- 50 J. R. Bernardo, F. M. Girio and R. M. Lukasik, *Molecules*, 2019, **24**, 17.
- 51 A. P. D. S. Morais, C. A. Sansigolo and M. D. O. Neto, *Bioresour. Technol.*, 2016, **214**, 623–628.
- 52 C. Brett and K. Waldron, *Physiology and Biochemistry of Plant Cell Wall*, Chapman & Hall, London, 1996.
- 53 T. Higuchi, *Biochemistry and Molecular Biology of Wood*, Springer, Berlin, 1997.
- 54 D. Fengel and G. Wegener, *Polyoses(Hemicelluloses), in Wood: Chemistry, Ultrastructure, Reactions*, 1984, pp. 106–131.
- 55 G. O. Aspinall, *Chemistry of cell wall polysaccharides, Biochem. Plants*, 1980, 473–500.
- 56 J. Sun, *Bioresour. Technol.*, 2012, **110**, 292–296.
- 57 X. Jiang, Q. Hou, W. Liu, H. Zhang and Q. Qin, *Bioresour. Technol.*, 2016, **222**, 361–366.
- 58 S. Cao, Y. Pu, M. Studer, C. Wyman and A. J. Ragauskas, *RSC Adv.*, 2012, **2**, 10925–10936.
- 59 M. Yoshida, Y. Liu, S. Uchida, K. Kawarada and K. Fukuda, *J. Agric. Chem. Soc. Jpn.*, 2008, **72**, 805–810.
- 60 P. Kavousi, H. Mirhosseini, H. Ghazali and A. A. Ariffin, *Food Chem.*, 2015, **182**, 164–170.
- 61 A. R. C. Morais, M. D. D. J. Matuchaki, J. Andreaus and R. Bogel-Lukasik, *Green Chem.*, 2016, **18**, 2985–2994.

